

PUBLISHED VERSION

ANTON BERGANT - ANGUS R. SIMPSON

Visualisation of transient cavitating flow in piping systems

Strojnicki Vestnik / Journal of Mechanical Engineering (Slovenia), 1996; 42(1-2):1-16

© Strojnicki Vestnik / Journal of Mechanical Engineering (Slovenia)

www.sv-jme.eu

PERMISSIONS

Email reply received 31 March 2015 from editor Strojnicki Vestnik / Journal of Mechanical Engineering (Slovenia)

PERMISSION FORM

to

*Litostroj Power
Ljubljana
Slovenia*

Hereby we grant you a non-exclusive permission for online publication of our original article as follows:

Bergant A, Simpson A. Visualisation of Transient Cavitating Flow in Piping Systems. Strojnicki Vestnik - Journal of Mechanical Engineering (Slovenia) 42(1-2):1-16 1996

at digital library of the University of Adelaide.

Please make sure that full acknowledgement will be given as well as the link to the sv-jme home page (www.sv-jme.eu).

STROJNIŠKI VESTNIK

JOURNAL OF MECHANICAL ENGINEERING

LETNIK 42
VOLUME

LJUBLJANA, JANUAR-FEBRUAR
1996
JANUARY-FEBRUARY

ŠTEVILKA 1-2
NUMBER

UDK 627.84:621.643:532.57

Vizualizacija kavitacijskega toka med prehodnimi režimi v cevnih sistemih Visualisation of Transient Cavitating Flow in Piping Systems

ANTON BERGANT -ANGUS R. SIMPSON

Članek obravnava vizualizacijo kavitacijskega toka med prehodnimi režimi v cevnih sistemih. Pretrganje kapljivinskega stebra v preizkusni postaji je posneto s hitro snemalnim video sistemom. Postaja je sestavljena iz poševnega cevovoda, ki je vgrajen med dva tlačna kotla. Dolžina cevovoda je 37,2 m, notranji premer je 22 mm. V cevovodu smo posneli diskretno parno kavitacijo in področje kontinuiranega kavitacijskega toka, ki nastaneta v primeru hitrega zaprtja ventila. Rezultati meritev (vizualizacija toka in meritev tlaka) so primerjani z rezultati, dobljenimi z diskretnim plinskim kavitacijskim modelom. Odstopanja med rezultati izračuna in meritev so minimalna.

The paper deals with the visualisation of transient cavitating flow in piping systems. A high-speed video-system is used to record liquid column separation events in an experimental apparatus. The apparatus comprises a straight 37.2 m long sloping pipeline of 22 mm internal diameter, connecting two pressurised tanks. A discrete vapour cavity and vaporous cavitation zone were observed in the pipeline following downstream end rapid valve closure. The results of measurements (flow visualisation and pressure measurement) are compared to the discrete gas cavity model results. There are minor discrepancies between the computed and measured results.

0 UVOD

Moderni hidravlični cevni sistemi delujejo v različnih prehodnih režimih, kakor so razbremene vodne turbine, izklop črpalke, zapiranje ventila itn. Zmanjšanje pretočne hitrosti v cevnem sistemu povzroči zvišanje tlaka. Po odboju vala od roba sledi padec tlaka. Teorija vodnega udara daje pravilne rezultate za tlak, večji od parnega tlaka kapljivine [1]. Kapljivinski steber se pretrga, ko se tlak zniža na parni tlak kapljivine. V področjih, kjer je tlak enak parnemu tlaku kapljivine, nadomestimo model vodnega udara z modelom pretrganja stebra [1] do [4]. Članek obravnava diskretni plinski kavitacijski model.

Pretrganje kapljivinskega stebra je z vztrajnostjo vzbujena hidrodinamična kavitacija. Predpostavimo zanemarljivo količino prostega in izločenega plina v kapljivini [1], [2], [5]. To velja za večino industrijskih sistemov. Obstajata dva tipa pretrganja stebra. Prvi je lokalna parna kavitacija z velikim kavitacijskim razmernikom. Drugi je področje kontinuiranega kavitacijskega toka vzdolž določene dolžine cevi. V tem primeru je kavitačijski razmernik majhen (blizu nič).

0 INTRODUCTION

Modern hydraulic pipeline systems run at a broad range of transient regimes i.e. water turbine load rejection, pump failure, valve closure, etc. A pipe flow velocity decrease in a piping system generates a pressure rise and subsequent pressure drop following wave reflection off the boundary. The water hammer theory gives valid results when the pressure is above the liquid vapour pressure [1]. If the pressure drops below the liquid vapour pressure, liquid column separation occurs. A column separation model [1] to [4] is used instead of the water hammer model for regions in the pipeline at which vapour pressure is detected. A discrete gas cavity model is presented in this paper.

Liquid column separation is inertial driven hydrodynamic cavitation assuming a negligible amount of free and released gas in the liquid [1], [2], [5]. This is usually the case in most industrial systems. Two types of column separation may occur. The first type is a localised vapour cavity with a large void fraction. The second is distributed vaporous cavitation, which may extend over long sections of the pipe. The void fraction for this case is small (close to zero).

Mehanizem pretrganja kapljevinskega stebra še ni povsem razjasnjen. Vizualizacija kavitacijskega toka med prehodnimi režimi v cevovodu lahko pomembno prispeva k boljšemu razumevanju pojava. Z vizualizacijo toka razberemo tip kavitacije (diskretna parna kavitacija, področje kontinuiranega kavitacijskega toka) in časovni razvoj dogodkov (nastanek in zrušitev kavitacije).

Prve študije z vizualizacijo toka pripisujemo Ducu [6] in O'Neillu [7]. Duc je fotografiral kavacijo v visokem kolenu črpalnega sistema po izklopu črpalki. O'Neill je fotografiral nastanek in zrušitev diskretne kavitacije vzdolž cevi po hitrem zaprtju ventila na navzdolnjem robu vodoravnega cevovoda. Isti avtor je vizualno opazil kavacijo pri ventilu (diskretna parna kavitacija) in številne majhne kavacije vzdolž cevi (področje kontinuiranega kavitacijskega toka). Diskretno kavacijo pri ventilu na navzgornjem robu preprostega cevnega sistema so posneli Li in Walsh [8], Baltzer [9] in Safwat [10]. Tanahashi in Kasahara [11] sta spremljala nastanek in zrušitev diskretne kavacije v visokem kolenu črpalnega sistema. Fotografije pretrganja kapljevinskega stebra v sesalni cevi vodne turbine pri naglem zapiranju vodilnika je podal Nonoshita s soavtorji [12]. Ugotovili so, da vrtinec v sesalni cevi turbine povzroči izločanje plina iz kapljevine in s tem tudi znižanje tlaka po zrušitvi diskretne kavacije. Swaffield [13] in Kojima s soavtorji [14] sta fotografirala pretrganje kapljevinskega stebra v kerozinu in mineralnem olju. Mehanizem pretrganja stebra je enak za vse vrste kapljevin.

Vizualizacija toka je v splošnem pokazala, da diskretna kavacija pri robu (zaprt ventil, visoko koleno) lahko zajame polni ali delni prečni prerez cevovoda. V področju kontinuiranega kavitacijskega toka so številne majhne kavacije, ki niso homogeno porazdeljene po prečnem prerezu cevovoda. Vse dosedanje fotografije pretrganja kapljevinskega stebra so bile posnete s hitro snemalno kamero. V tem članku je podana nova tehnika vizualizacije pretrganja stebra. Hitro snemalni video omogoča vizualizacijo celotnega dogodka pretrganja stebra in s tem tudi boljše razumevanje zaporedja hitrih dogodkov.

Snemanje pretrganja kapljevinskega stebra s hitro snemalnim video sistemom je bilo izvedeno na preizkusni postaji. Postaja je sestavljena iz poševnega cevovoda, ki je vgrajen med dva tlačna kotla. Dolžina cevovoda je 37,2 m, notranji premer je 22 mm. V cevovodu smo posneli diskretno parno kavacijo in področje kontinuiranega kavitacijskega toka, ki nastaneta v primeru hitrega zaprtja ventila na navzdolnjem robu. Izследki s fotografij, dobljeni s hitro snemalnim video sistemom, in rezultati meritev tlaka so primerjani z rezultati izračuna po diskretnem plinskem kavitacijskem modelu.

The mechanism of liquid column separation is not yet fully understood. Visualisation of transient cavitating pipe flow may significantly contribute to better understanding of the phenomenon. Flow visualisation detects the type of cavitation (discrete vapour cavity or distributed vaporous cavitation zone) and time sequence of events (evolution of the formation and collapse of the cavity).

Early flow visualisation studies were reported by Duc [6] and O'Neill [7]. Duc photographed a discrete cavity at a high point of a pumping system following pump failure. O'Neill photographed the formation and collapse of an intermediate cavity in a horizontal pipeline following closure of a downstream end valve. He visually observed a large cavity at the valve (discrete vapour cavity) and several small cavities along the pipeline (distributed vaporous cavitation zone). Li and Walsh [8], Baltzer [9], and Safwat [10] presented photographs of a discrete cavity at the downstream side of an upstream end closing valve in a simple pipeline system. Tanahashi and Kasahara [11] studied the formation and collapse of a discrete cavity at the high point of a pumping system. Nonoshita et al. [12] presented photographs of liquid column separation in a draft tube of a water turbine following wicket gates closure. In addition, the effect of the draft tube inlet swirl flow on column separation was studied. The swirl flow generates gas release and subsequent attenuation of maximum pressure following discrete cavity collapse. Swaffield [13] and Kojima et al. [14] employed photography to visualise column separation in liquids other than water (kerosine, mineral oil). No differences in the column separation mechanism in various liquids were observed.

Generally, previous flow visualisation studies have shown that a discrete vapour cavity at a boundary (closed valve, high point) may or may not occupy the entire pipe cross-section. Small cavities were observed in a distributed vaporous cavitation zone. The cavities were not homogeneously distributed in the pipe cross-section. All reported flow visualisation studies of liquid column separation have been carried out by a high-speed camera. A new observation technique is proposed in this paper. High-speed video enables observation of the evolution of the entire event of column separation and should thus lead to a better understanding of the sequence of high-speed events.

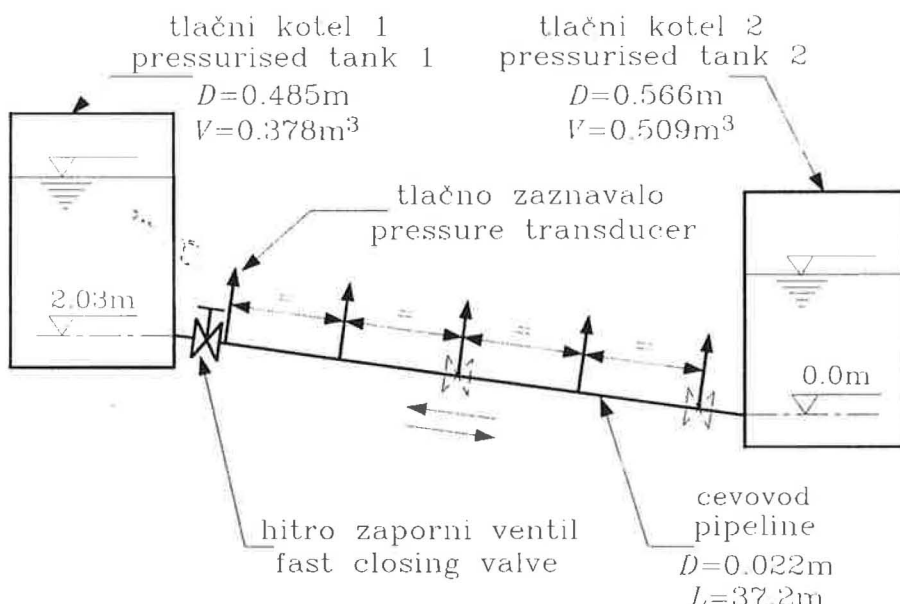
A high-speed video-system was used to record liquid column separation events in an experimental apparatus. The apparatus comprises a straight 37.2 m long sloping pipeline of 22 mm internal diameter, connecting two pressurised tanks. A discrete vapour cavity and vaporous cavitation zone were observed following downstream end rapid valve closure. The results obtained from the high-speed video-system photographs and pressure measurements are compared to the discrete gas cavity model results.

1 PREIZKUSNA POSTAJA

Preizkusna postaja za raziskave vodnega udara in kavitacijskega toka v cevnih sistemih je instalirana v Robinovem hidravličnem laboratoriju Oddelka za gradbeništvo in varstvo okolja Univerze v Adelaidi, Avstralija. Postaja je sestavljena iz poševnega cevovoda, ki je vgrajen med tlačna kotla (sl. 1). Največji dovoljeni tlak v cevovodu je 5 MPa in v tlačnih kotlih 690 kPa. Pretočni medij je demineralizirana voda. Podrobni opis postaje je podan v [2] in [15].

1 EXPERIMENTAL APPARATUS

The experimental apparatus for investigating water hammer and column separation events in pipelines is located in the Robin Hydraulic Laboratory at the Department of Civil and Environmental Engineering, University of Adelaide, Australia. The apparatus comprises a straight sloping pipeline connecting two pressurised tanks (Fig. 1). The design pressure of the pipeline is 5 MPa, while for the pressurised tanks it is 690 kPa. Demineralised water is used as the fluid. Details of the apparatus are given in [2] and [15].



Sl. 1. Preizkusna postaja
Fig. 1. Experimental apparatus

Meritev v preizkusni postaji poteka v dveh fazah. V prvi dosežemo želene ustaljene pretočne razmere v cevovodu. V drugi fazi hitro zapiranje ventila vzbudi vodni udar in pretrganje kapljevinskega stebra. Ventil je lahko vgrajen ob tlačnih kotlih ali na polovici dolžine cevovoda. Lokacija ventila omogoča simuliranje poljubnega hidravličnega sistema (pretočni sistem hidroelektrarne, črpalni sistem itn.). Ventil je zaprt ročno ali z zapiralnim mehanizmom s torzijsko vzmetjo (čas zapiranja ventila je krajši od 0,01 s). Elektronska regulacija tlaka v obeh kotlih zagotavlja poljubno smer pretoka v cevovodu in s tem tudi študij prehodnih pojavov v cevovodu s pozitivno ali negativno strmino. Koristna prostornina vode v tlačnih kotlih in zmogljivost kompresorja omejujeta največjo pretočno hitrost v cevovodu na 1,5 m/s in največji tlak (višino) v obeh kotlih na 400 kPa (40 m).

Each experiment using the column separation apparatus consists of two phases. First, an initial steady state velocity condition is established in the pipeline. Second, a water hammer and liquid column separation event is initiated by rapid closure of a valve. The valve can be located at either end of the pipeline, adjacent to either tank, or at the midpoint of the pipeline. As a consequence, the experimental simulation of various types of hydraulic systems (hydroelectric power plant, pumping system, etc.) may be performed. The valve may be closed by a torsional spring actuator (valve closure time less than 0.01 s) or manually by hand. A pressure control system for maintaining specified pressure in each of the tanks enables the flow in the pipeline to be in either direction. Transient behaviour in both an upward and downward sloping pipe can thus be studied. The net water volume in both tanks and the capacity of the air compressor limit the maximum steady state velocity to 1.5 m/s and maximum pressure (head) in each tank to 400 kPa (40 m).

Neposredno merjene ustaljene veličine so tlak v obeh kotlih ($U_x = \pm 0,3\%$), barometrski tlak ($U_x = \pm 0,1\text{ kPa}$) in temperatura zraka ($U_x = \pm 0,5\text{ }^{\circ}\text{C}$), kjer je nezanesljivost meritve U_x izražena kot koren vsote kvadratov sistemskega in naključnega pogreška [15], [16]. Veličine, merjene v odvisnosti od časa, so tlaki na petih ekvidistantnih mestih vzdolž cevovoda ($U_x = \pm 0,7\%$ za piezoelektrična tlačna zaznavala, $U_x = \pm 0,3\%$ za induktivna tlačna zaznavala), čas zapiranja ventila ($U_x = \pm 0,0001\text{ s}$) in temperatura vode ($U_x = \pm 0,5\text{ }^{\circ}\text{C}$). Meritev je registrirana z merilnim računalnikom Concurrent 6655. Ustaljena pretočna hitrost v cevovodu je dobljena posredno s prostorninsko metodo ($U_x = \pm 1\%$) in metodo vodnega udara ($U_x = \pm 0,7\%$). Hitrost širjenja udarnih valov ($U_x = \pm 0,1\%$) je določena iz časa potovanja primarnega udarnega vala med ventilom in bližnjo četrtino dolžine cevovoda.

Ob hitro zapornem ventilu je vgrajen prozorni polikarbonatni del cevovoda. Razvoj nastanka in zrušitve parnih kavitacij smo posneli s hitro snemalnim sistemom. Podrobni oris hitro snemalnega video sistema je podan v naslednjem poglavju.

2 VIZUALIZACIJA TOKA

Vizualizacijo kavitacijskega toka med prehodnimi režimi v cevnih sistemih smo izvedli s hitro snemalnim video sistemom (sl. 2). Sistem sestavlja prozorni del cevovoda, svetilo (močan svetlobni vir) in hitro snemalni video Kodak Ektapro 1000. Največja hitrost snemanja je 1000 slik na sekundo.

Ob hitro zapornem kroglastem ventilu je vgrajen prilagodljiv (zamenljiv) polikarbonatni del (Lexan), dolžine 150 mm in z notranjim premerom 22 mm. V fazi testiranja je bil prozorni del vgrajen tudi na polovici dolžine cevovoda. Del, vgrajen na polovici dolžine cevovoda, vzbudi neželeno interakcijo med tekočino in konstrukcijo. Prozorni del na polovici dolžine cevovoda smo zato zamenjali z delom iz brona [17].

Prozorni polikarbonatni del je osvetljen s svetilom ILC PS300-1 (300 W ksenon-obločna žarnica). Snop svetlobe v vodoravni ravnini se odbije od ogledala v navpično ravnino. Navpični snop svetlobe osvetljuje prozorni polikarbonatni del skozi nastavljivo režo na spodnji strani škatle, ki je pritrjena na ogrodje prozornega dela. Usmerjeni snop svetlobe omogoča natančno lokacijo kavitacije v vzdolžnem prerezu cevi. Moč svetlobe dovoljuje 250 posnetkov na sekundo. Avtorja načrtujeva gradnjo laserskega vira svetlobe za večje število posnetkov. Tanek snop svetlobe dobimo z razpršitvijo laserskega žarka v ravnino [18]. Uporabi svetlobe v vodoravni ravnini smo se izognili zaradi učinkov senčenja in možnosti poškodbe optičnega zaznavala v hitro snemalni video kamери.

The directly measured steady state quantities are the pressure in each tank ($U_x = \pm 0.3\%$), barometric pressure ($U_x = \pm 0.1\text{ kPa}$) and ambient temperature ($U_x = \pm 0.5\text{ }^{\circ}\text{C}$), in which the uncertainty in a measurement U_x is expressed as a root-sum-square combination of bias and precision errors [15], [16]. The time dependent quantities are pressures at 5 equidistant points along the pipeline ($U_x = \pm 0.7\%$ for piezoelectric pressure transducers, $U_x = \pm 0.3\%$ for strain-gauge pressure transducers), valve closure time ($U_x = \pm 0.0001\text{ s}$) and water temperature ($U_x = \pm 0.5\text{ }^{\circ}\text{C}$). Data acquisition is performed with a Concurrent 6655 data acquisition computer. The initial steady state velocity in the pipeline is measured indirectly by the volumetric method ($U_x = \pm 1\%$) and the water-hammer method ($U_x = \pm 0.7\%$). The wave propagation velocity ($U_x = \pm 0.1\%$) is obtained from the measured time for a water-hammer wave to travel between the closed valve and the quarter point nearest the valve.

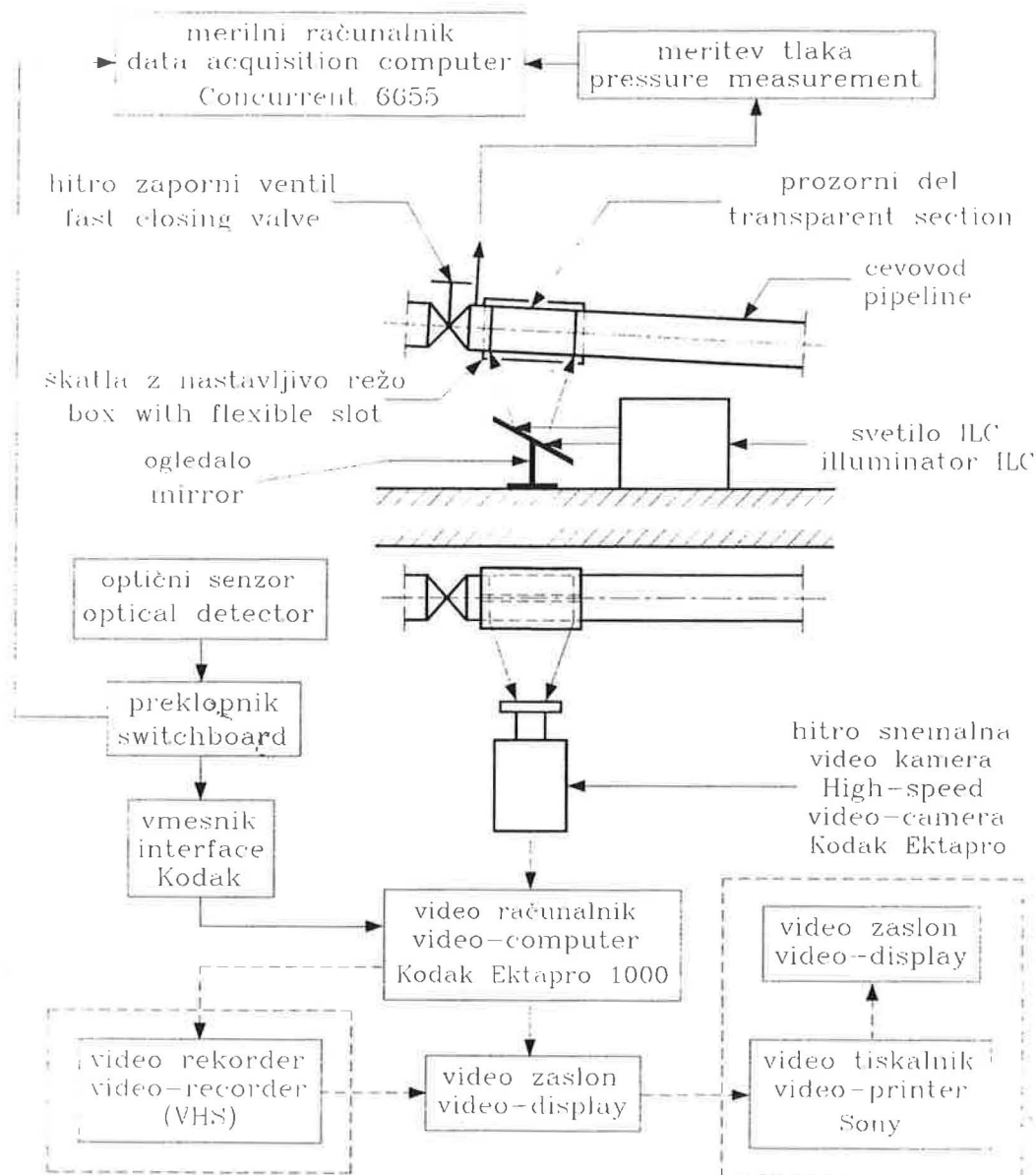
The flow visualisation polycarbonate section is positioned adjacent to the fast closing valve. A high-speed video was used to record the evolution of the formation and collapse of vapour cavities. Details of the high-speed video-system are given in the following section.

2 FLOW VISUALISATION

A sophisticated high-speed video-system for visualisation of transient cavitating flow in piping systems has been developed (Fig. 2). The system is comprised of a flow visualisation pipe section, high intensity illuminator and high-speed video Kodak Ektapro 1000. The maximum rate for the high-speed video is 1000 frames per second.

The flexible (removable) flow visualisation polycarbonate (Lexan) section of 150 mm length and 22 mm internal diameter was positioned adjacent to the fast closure ball valve. Another flow visualisation section was positioned at the midpoint of the pipeline. After initial tests and subsequent investigations, the central polycarbonate section was removed due to fluid-structure interaction effects on the transient event, and replaced by a brass insert [17].

The polycarbonate section is illuminated by a high intensity illuminator ILC PS300-1 (Xenon arc lamp of 300 W). A horizontal light beam is reflected off the mirror in a vertical direction. The vertical directed light illuminates the transparent polycarbonate section via a flexible slot at the bottom of the box which is fixed to the flow visualisation block. A plane sheet of light enables accurate location of cavities in a longitudinal cross section of the pipe. The intensity of light allows 250 frames per second. The authors are planning to build a laser illuminating system for a higher frame rate. A thin sheet of light can be obtained by expanding the laser beam in one plane [18]. The use of a horizontal light beam was omitted due to shading effects and the probable deterioration of the optical sensor in a high-speed video-camera.



Sl. 2. Hitro snemalni video sistem
Fig. 2. High-speed video-system

Elementi hitro snemalnega videa Kodak Ektapro 1000 so hitro snemalna videokamera, video računalnik in video zaslon. Hitro snemalna video kamera spremeni optični signal v električnega, ki se shrani v hitro snemalni video kaseti video računalnika. Kavitacijski pojav opazujemo na video zaslonu neposredno med meritvijo ali pa s predvajanjem po meritvi. Časovna ustreznost posnetih dogodkov z meritvami, registriranimi z računalnikom Concurrent (tlak, čas zapiranja ventila, temperatura vode) je dobljena s povezavo hitro snemalnega videa prek vmesnika na preklopnik (sl. 2). Ta registrira lego ventila med zapiranjem. Začetek (start) prehodnega procesa je tako označen na hitro snemalni video kaseti.

The high-speed video Kodak Ektapro 1000 is comprised of high-speed video-camera, video-computer and video-display. The high-speed video-camera converts the optical signal into an electrical signal which is then recorded on the high-speed video-cassette in the video-computer. Cavitation photography is monitored directly on the video-display (monitor) during the experiment or during play-back after the experiment. Time compatibility of the high-speed video photography with the measurements recorded by the Concurrent computer (pressure, valve closure time, water temperature) is obtained by connecting the high-speed video via a Kodak interface to the switchboard (Fig. 2). The switchboard registers the valve position following valve closure. The initiation (start) of the transient is recorded on the Kodak high-speed video-cassette.

Posamezno sliko na zaslonu hitro snemalnega videa Kodak Ektapro 1000 dobimo v obliki fotografije s prenosom slike na video tiskalnik Sony Mavigraph UP-5000P. Kavitacijski pojav posnet na hitro snemalni video kaseti Kodak lahko prenesemo na standardno VHS video kaseto. Iz-sledki s fotografij kavitacijskega toka, dobljenimi s hitro snemalnim videom, so podani v poglavju 4.

3 TEORETIČNI MODEL

Natančna določitev največjih tlakov po zrušitvi kavitacije je pomembna za ekonomično načrtovanje cevnih sistemov. Diskretni parni kavitacijski model [19] je najpogosteje uporabljan model v računalniških paketih, dostopnih na trgu. Rezultati izračuna, dobljeni z diskretnim parnim kavitacijskim modelom, niso vedno dovolj natančni [2], [4]. Boljši v primerjavi z diskretnim parnim kavitacijskim modelom je diskretni plinski kavitacijski model ob uporabi dovolj majhnega plinskega kavitacijskega razmernika ($\alpha_0 \leq 10^{-7}$) [20], [21]. Diskretni plinski kavitacijski model daje dovolj natančne rezultate za širok spekter podatkov [2], [4].

3.1 Model vodnega udara

Nestacionarni tok v cevovodu (vodni udar) popišemo s kontinuitetno in gibalno enačbo v eni izmeri [1]:

$$\frac{\partial H}{\partial t} + v \frac{\partial H}{\partial x} - v \sin \theta + \frac{a^2}{g} \frac{\partial v}{\partial x} = 0 \quad (1)$$

$$g \frac{\partial H}{\partial x} + \frac{\partial v}{\partial t} + v \frac{\partial v}{\partial x} + \frac{\lambda v |v|}{2D} = 0 \quad (2)$$

Konvekcijski členi v enačbah (1) in (2) so majhni in jih zato običajno zanemarimo. Standardna metoda za reševanje enačb vodnega udara je metoda karakteristik. Enočbi (1) in (2) preoblikujemo v dva para kompatibilnih enačb vodnega udara in enačb karakterističnih krivulj. Te enačbe se v obliki končnih razlik v numeričnem vozlišču vzdolž cevovoda j v času t glase (majhne člene zanemarimo) [1]:

— kompatibilnostna enačba vodnega udara vzdolž karakteristike C^+ ($\Delta x / \Delta t = a$):

$$H_{j,t} - H_{j-1,t-\Delta t} + \frac{a}{g} \left[(v_u)_{j,t} - v_{j-1,t-\Delta t} \right] + \frac{\lambda \Delta x}{2gD} v_{j,t} \left| v_{j-1,t-\Delta t} \right| = 0 \quad (3)$$

Each frame may be recovered as a photograph by connecting the high-speed video Kodak Ektapro 1000 to the video-printer Sony Mavigraph UP-5000P. Cavitation phenomena recorded on the Kodak high-speed video-cassette may also be transferred to a standard VHS video-cassette. The results of high-speed video transient cavitation flow photography are given in section 4.

3 THEORETICAL MODEL

The accurate prediction of maximum pressures following cavity collapse is important for the economic design of piping systems. A commonly used model in commercially available software is the discrete vapour cavity model [19]. Numerical studies have indicated that results from the discrete vapour cavity model are inconsistent [2], [4]. An improved model (compared to the discrete vapour cavity model) is a discrete gas cavity model using a low gas void fraction ($\alpha_0 \leq 10^{-7}$) [20], [21]. The discrete gas cavity model performs consistently over a broad range of parameters [2], [4].

3.1 Water-hammer model

Unsteady flow in pipelines (water-hammer) is described by an one-dimensional equation of continuity and motion [1]:

The pipe slope and convective acceleration terms in equations (1) and (2) are small and usually neglected. The method of characteristics is the standard procedure for solving water-hammer equations. The equations (1) and (2) are transformed into the following two pairs of water-hammer compatibility equations and characteristic curve equations written in a finite-difference form at a computational node j at time t along the pipeline (small terms are neglected) [1]:

— water hammer compatibility equation along the C^+ characteristic line ($\Delta x / \Delta t = a$):

— kompatibilnostna enačba vodnega udara vzdolž karakteristike C^- ($\Delta x/\Delta t = -a$):

$$H_{j,t} - H_{j+1,t-\Delta t} - \frac{a}{g} \left[v_{j,t} - (v_u)_{j+1,t-\Delta t} \right] - \frac{\lambda \Delta x}{2gD} v_{j,t} \left| (v_u)_{j+1,t-\Delta t} \right| = 0 \quad (4).$$

V enačbah (3) in (4) običajno uporabimo konstantno vrednost Darcy-Weisbachovega koeficiente trenja λ [22]. Neznanke v sistemu enačb (3) in (4) so piezometrična višina $H_{j,t}$, vstopna hitrost $(v_u)_{j,t}$ in izstopna hitrost $v_{j,t}$ v numeričnem vozlišču j . Za kapljevinski tok sta hitrosti enaki: $(v_u)_{j,t} \equiv v_{j,t}$. Sistem enačb rešujemo algebroično z eliminacijo neznanke.

Na robu enačba robnega pogoja nadomesti eno od kompatibilnostnih enačb vodnega udara. Robna pogoja za računski primer v poglavju 4 (cevni sistem s pozitivno strmino po sliki 1) sta navzgornji kotel s konstantno gladino vode (numerično vozlišče $j = 1$, piezometrična višina H_{ur}) in ventil priključen na navzdoljni kotel (numerično vozlišče $j = N + 1$, piezometrična višina H_{dr}). Pretočno hitrost pri navzgornjem kotlu $v_{1,t}$ izračunamo iz enačbe (4) pri predpostavki $H_{1,t} = H_{ur}$. Piezometrično višino $H_{N+1,t}$ in pretočno hitrost $v_{N+1,t}$ na navzgornji strani ventila, priključenega na navzdoljni kotel izračunamo iz enačbe (3), kjer je $(v_u)_{N+1,t} \equiv v_{N+1,t}$, in običajne enačbe za ventil [1], [23]:

$$v_{N+1,t} = \frac{v_{N+1,0}}{\sqrt{H_{N+1,0} - H_{dr}}} \tau \sqrt{H_{N+1,t} - H_{dr}} \quad (5),$$

kjer je brezdimenzijsko odprtje ventila τ izraženo z enačbo:

$$\tau = \tau_i - (\tau_i - \tau_f) \left(\frac{t}{t_c} \right)^\beta \quad (6).$$

V obravnavanem numeričnem modelu uporabimo deltoidno mrežo v metodi karakteristik [1], [2]. V prvem koraku izračunamo ustaljene pretočne razmere v času $t = 0$. V računalniški programske zanki za izračun prehodnih pojavov najprej izračunamo pretočne razmere v numeričnih vozliščih vzdolž cevovoda, označenih s sodo številko (časovni korak $(2n + 1)\Delta t$, kjer je n celo število) in nato v numeričnih vozliščih, označenih z liho številko (časovni korak $2(n + 1)\Delta t$). Temu sledi izračun robnih pogojev (navzgornji kotel, ventil na navzdolnjem koncu) v cevovodu (časovni korak $2\Delta t$).

Kapljevinski steber v cevovodu se pretrga, ko tlak kapljevine pada na parni tlak kapljevine.

— water-hammer compatibility equation along the C^- characteristic line ($\Delta x/\Delta t = -a$):

$$H_{j,t} - H_{j+1,t-\Delta t} - \frac{a}{g} \left[v_{j,t} - (v_u)_{j+1,t-\Delta t} \right] - \frac{\lambda \Delta x}{2gD} v_{j,t} \left| (v_u)_{j+1,t-\Delta t} \right| = 0 \quad (4).$$

A constant value of the Darcy-Weisbach friction factor λ is usually used in equations (3) and (4) [22]. The unknowns in the system of equations (3) and (4) are piezometric head $H_{j,t}$, upstream velocity $(v_u)_{j,t}$ and downstream velocity $v_{j,t}$. At node j , however, the velocities are equal for the liquid flow: $(v_u)_{j,t} \equiv v_{j,t}$. The system of equations is solved algebraically by elimination of a unknown.

At a boundary, the boundary equation replaces one of the water hammer compatibility equations. The upstream reservoir with constant water level (node number $j = 1$, piezometric head H_{ur}) and a downstream end valve adjacent to the reservoir (node number $j = N + 1$, piezometric head H_{dr}) are the boundary conditions for the computational example presented in Section 4 (upward sloping pipe system in Fig. 1). The flow velocity at the upstream reservoir $v_{1,t}$ is calculated from equation (4) assuming $H_{1,t} = H_{ur}$. Piezometric head $H_{N+1,t}$ and flow velocity $v_{N+1,t}$ at the upstream side of the downstream end valve are calculated from equation (3) in which $(v_u)_{N+1,t} \equiv v_{N+1,t}$ and standard valve equation [1], [23]:

in which the dimensionless valve opening τ is expressed by the equation:

$$\tau = \tau_i - (\tau_i - \tau_f) \left(\frac{t}{t_c} \right)^\beta \quad (6).$$

The staggered grid in the method of characteristics is used in the numerical model described in this paper [1], [2]. First, the computation of steady state flow conditions is carried out at time $t = 0$. In the transient loop within the computer program, the computation of the even numbered pipe interior nodes at the time step $(2n + 1)\Delta t$ and the odd numbered pipe nodes at the time step $2(n + 1)\Delta t$ is first carried out. Computation of the pipe end boundary conditions (upstream end reservoir, downstream end valve) follows at every $2\Delta t$ time steps.

When the pressure head in a pipeline system drops below the liquid pressure head, liquid column

Pretrganje stebra je lahko v obliki diskretne parne kavitacije ali kontinuiranega kavitacijskega toka pri parnem tlaku kapljevine [2], [3], [24]. Diskretni plinski kavitacijski model nadomesti model vodnega udara, ki velja za kapljevinski tok (enokomponentni enofazni tok). Diskretni plinski kavitacijski model simulira dvokomponentni dvofazni tok. Z obravnavanim modelom tudi natančno izračunamo vodni udar, ko izberemo dovolj majhen plinski kavitacijski razmernik ($\alpha_0 \leq 10^{-7}$) pri referenčni tlačni višini h_0^* . Diskretni plinski kavitacijski model simulira tako vodni udar kakor kavitacijski tok med prehodnimi režimi v cevnih sistemih.

3.2 Diskretni plinski kavitacijski model

Diskrette plinske kavitacije so vgrajene v vseh numeričnih vozliščih v deltoidni mreži metode karakteristik. V cevnih odsekih med numeričnimi vozlišči obstaja kapljevinski tok. Diskretna plinska kavitačija v numeričnem vozlišču j v času t je popisana z dvema kompatibilnostnima enačbama vodnega udara (3) in (4), plinsko enačbo (izotermni proces):

$$(H_{j,t} - z_j - h_v)(V_g)_{j,t} = h_0^* \alpha_0 A \Delta x$$

in integrirano kontinuitetno enačbo diskrette plinske kavitačije v deltoidni mreži metode karakteristik [1], [2], [21]:

$$(V_g)_{j,t} = (V_g)_{j,t-2\Delta t} + \left\{ \psi \left[v_{j,t} - (v_u)_{j,t} \right] + (1-\psi) \left[v_{j,t-2\Delta t} - (v_u)_{j,t-2\Delta t} \right] \right\} A 2\Delta t \quad (8)$$

Vrednost utežnega koeficiente ψ je od 0,5 do 1. Neznane v sistemu enačb (3), (4), (7) in (8) so piezometrična višina $H_{j,t}$, vstopna hitrost v vozlišče $(v_u)_{j,t}$, izstopna hitrost iz vozlišča $v_{j,t}$ in prostornina diskrette plinske kavitačije $(V_g)_{j,t}$. Sistem enačb rešujemo algebraično z eliminacijo neznank. Izračun prostornine diskrette plinske kavitačije po enačbi (8) ponovimo, ko je izračunana prostornina po enačbi (7) negativna.

Diskretni plinski kavitacijski model, uporabljen za računski primer v poglavju 4 modificiramo na robovih. Kavitačija ne obstaja pri navzgornjem kotlu (vodni udar). Pri hitro zapornem ventilu ($t_c < 2L/a$) na navzdolnjem koncu cevi diskretno plinsko kavitačijo zamenjamo z diskretno parno kavitačijo (velika kavitačija pri parni tlačni višini [2]). Nastanek diskrette parne kavitačije je odvisen od zmanjšanja tlačne višine na parno tlačno višino kapljevine. Diskretno parno kavitačijo pri zaprtem ventilu popišemo s kompatibilnostno enačbo vodnega udara (3), kjer je

separation occurs either as a discrete vapour cavity or vaporous cavitation zone [2], [3], [2]. The standard water hammer solution which valid for liquid flow (one-component one-phase flow) is replaced by a discrete gas cavity model. The discrete gas cavity model simulates two-component two-phase flow. In addition, discrete gas cavity model accurately predicts water-hammer if a small gas void fraction ($\alpha \leq 10^{-7}$) at the reference pressure h_0^* is selected in the model. The model thus simulates water-hammer and transient cavitating flow in pipe systems.

3.2 Discrete gas cavity model

The discrete gas cavities are lumped at computing nodes within the staggered grid of the method of characteristics. The liquid is assumed to occupy the full reach length between computational nodes. The discrete gas cavity at a computational nodes j at time t in the pipeline is fully described by the two water-hammer compatibility equations (3) and (4), the equation of the ideal gas (isothermal process):

and the integrated continuity equation for the discrete gas cavity within the staggered grid of the method of characteristics [1], [2], [21]:

The weighting factor ψ takes on values between 0.5 and 1. The unknowns in the system of equations (3), (4), (7) and (8) are piezometric head $H_{j,t}$, upstream velocity at node $(v_u)_j$, downstream velocity at node $v_{j,t}$ and discrete gas cavity volume $(V_g)_{j,t}$. The system of equations is solved algebraically by elimination of unknowns. When the discrete gas cavity volume computed by equation (8) becomes negative, the cavity volume is recalculated by equation (7).

The discrete gas cavity model is modified for the two boundaries for the computational example in Section 4. There is no cavity at the upstream end reservoir (water-hammer computations). A downstream end fast closing valve ($t_c < 2L/a$) in the discrete gas cavity is replaced by a discrete vapour cavity (large cavity with vapour pressure head). A discrete vapour cavity forms when the pressure head drops to the liquid vapour pressure head. The discrete vapour cavity at the closed valve is fully described by a water-hammer compatibility equation (3).

$H_{N+1,t} = z_{N+1} + h_v$, in integrirano kontinuitetno enačbo diskretne parne kavitacije v deltoidni mreži metode karakteristik [2]:

$$(V_v)_{N+1,t} = (V_v)_{N+1,t-2\Delta t} + [\psi(v_u)_{N+1,t} + (1-\psi)(v_u)_{N+1,t-2\Delta t}] A 2\Delta t \quad (9).$$

Kapljevinski tok se ponovno vzpostavi po zrušitvi kavitacije pri ventilu (negativna prostornina kavitacije). Piezometrično višino $H_{N=1,t}$ izračunamo iz enačbe (3), kjer je $(v_u)_{N+1,t} = v_{N+1,t} = 0$.

4 PRIMERJAVA REZULTATOV IZRAČUNA IN MERITEV

Primerjava rezultatov izračuna z meritvami tlaka in fotografijami kavitacije zagotavlja solidno podlago za overitev postavk v diskretnem plinskom kavitacijskem modelu in prispeva k boljšemu razumevanju pojava pretrganja kapljevinskega stebra. Tu obravnavamo primer zapiranja ventila, ki je vgrajen na navzdolnjem koncu cevovoda s pozitivno strmino (sl. 1). Pretočne razmere so:

- ustaljena pretočna hitrost $v_0 = 1,50 \text{ m/s}$,
- piezometrična višina v navzgornjem tlačnem kotlu $H_{ur} = 22 \text{ m}$,
- čas zapiranja ventila $t_c = 0,009 \text{ s}$ in
- hitrost širjenja udarnih valov $a = 1319 \text{ m/s}$.

V numerični analizi smo izbrali naslednje parametre:

- število cevnih odsekov $N = 16$,
- utežni koeficient $\psi = 1$ in
- plinski kavitacijski razmernik pri referenčni tlačni višini (barometrična tlačna višina) $\alpha_0 = 10^{-7}$.

Izmerjeni tlaki so podani kakor piezometrične višine z osnovnico na vrhu cevi, priključene na kotel 2 (kota 0,0 m na sliki 1). Frekvenca zbranih podatkov za vsako izmerjeno veličino v preizkusni postaji je $f_s = 5 \text{ kHz}$. Primerjamo časovni potek (t) piezometričnih višin na navzgornji strani hitro zapornega ventila H_{dv} in polovici dolžine cevovoda H_{mp} . Višini sta izmerjeni s piezoelektričnim tlačnim zaznavalom Kistler 603 B. Višina ob navzgornjem tlačnem kotlu je konstantna. Višini, izmerjeni na četrtinah dolžine cevovoda sta podobni višini na polovici dolžine cevovoda.

Izmerjeni in izračunani piezometrični višini pri ventili H_{dv} in na polovici dolžine cevovoda H_{mp} sta primerjani na slikah 3 in 4. Največja višina v cevnem sistemu je višina vodnega udara pri ventilu (sl. 3). Izračunana največja višina je enaka izmerjeni največji višini ($H_{dv})_{max} = 224 \text{ m}$. Najmanjša višina vzdolž cevovoda je enaka parni tlačni višini kapljevine $h_v = -10,3 \text{ m}$ (sl. 3, 4). Izračunani čas obstoja prve diskretne kavitacije pri ventilu $t = 0,331 \text{ s}$ se razlikuje od izmerjenega časa $t = 0,339 \text{ s}$ za 2,5 odstotka. Za drugo, tretje

in which $H_{N+1,t} = z_{N+1} + h_v$ and the integrated continuity equation of the discrete vapour cavity volume within the staggered grid of the method of characteristics [2]:

$$(V_v)_{N+1,t} = (V_v)_{N+1,t-2\Delta t} + [\psi(v_u)_{N+1,t} + (1-\psi)(v_u)_{N+1,t-2\Delta t}] A 2\Delta t \quad (9).$$

When the cavity at the closed valve collapses (negative cavity volume) then the liquid flow is reestablished. The piezometric head $H_{N=1,t}$ is calculated from equation (3) in which $(v_u)_{N+1,t} = v_{N+1,t} = 0$.

4 COMPARISON OF COMPUTATIONAL RESULTS WITH MEASUREMENTS

Comparison of computational results with pressure measurements and high-speed video photography should give satisfactory verification of the performance of the discrete gas cavity model and a better understanding of liquid column separation phenomena. The results for the closure of a downstream end valve in an upward sloping pipe (Fig. 1) are presented in this paper. The flow conditions are:

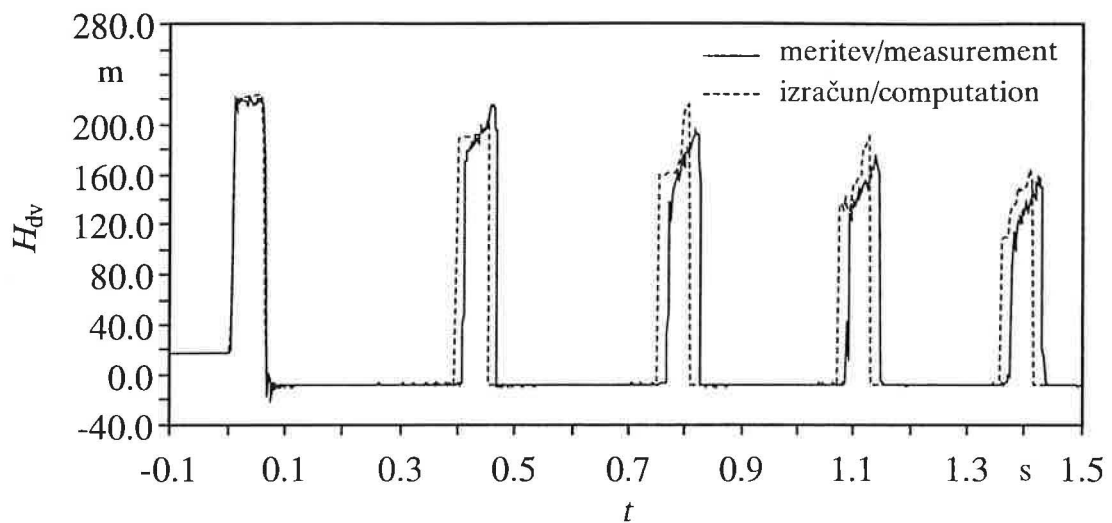
- initial flow velocity $v_0 = -1.50 \text{ m/s}$,
- piezometric head in the upstream end pressurised tank $H_{ur} = 22 \text{ m}$,
- valve closure time $t_c = 0.009 \text{ s}$, and
- wave propagation velocity $a = 1319 \text{ m/s}$.

The following parameters have been selected in the numerical analysis:

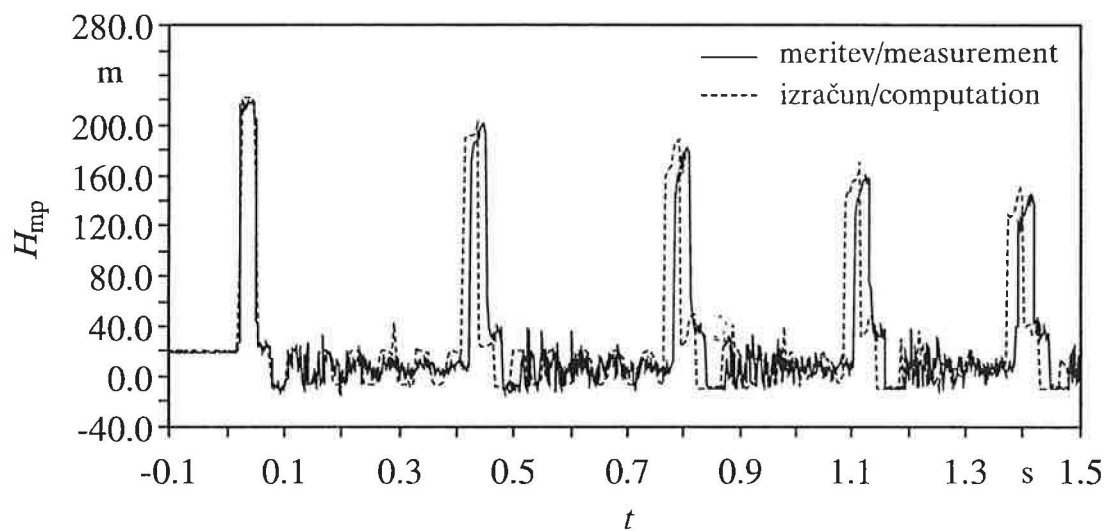
- number of reaches in pipeline $N = 16$,
- weighting factor $\psi = 1$, and
- gas void fraction at reference pressure head (barometric pressure head) $\alpha_0 = 10^{-7}$.

Measured pressures are given as piezometric heads with a datum level at the top of the pipe at tank 2 (elevation 0.0 m in Fig. 1). The sampling frequency for each measured quantity in the experimental apparatus is $f_s = 5 \text{ kHz}$. A comparison of the piezometric heads at the upstream side of the fast closing valve H_{dv} and at the midpoint of the pipeline H_{mp} versus time t is presented. The two heads are measured by Kistler 603 B piezoelectric type pressure transducers. The head at the upstream end tank 2 is constant, whereas the heads at the quarter points are similar to the head at the midpoint of the pipeline.

Measured and computed piezometric heads at the valve H_{dv} and at the midpoint of the pipeline H_{mp} are compared in Figs. 3 and 4, respectively. The maximum head that occurs in the pipeline system is the water-hammer head at the valve (Fig. 3). The computed maximum head matches the measured head $(H_{dv})_{max} = 224 \text{ m}$. The minimum head that occurs in the pipeline is the liquid vapour pressure head $h_v = -10.3 \text{ m}$ (Figs. 3, 4). The computed time of the length of the first cavity existence at the valve $t = 0.331 \text{ s}$ differs from the measured time $t = 0.339 \text{ s}$, representing a 2.5 %



Sl. 3. Primerjava piezometričnih višin H_{dv} pri ventilu
Fig. 3. Comparison of piezometric heads H_{dv} at the valve



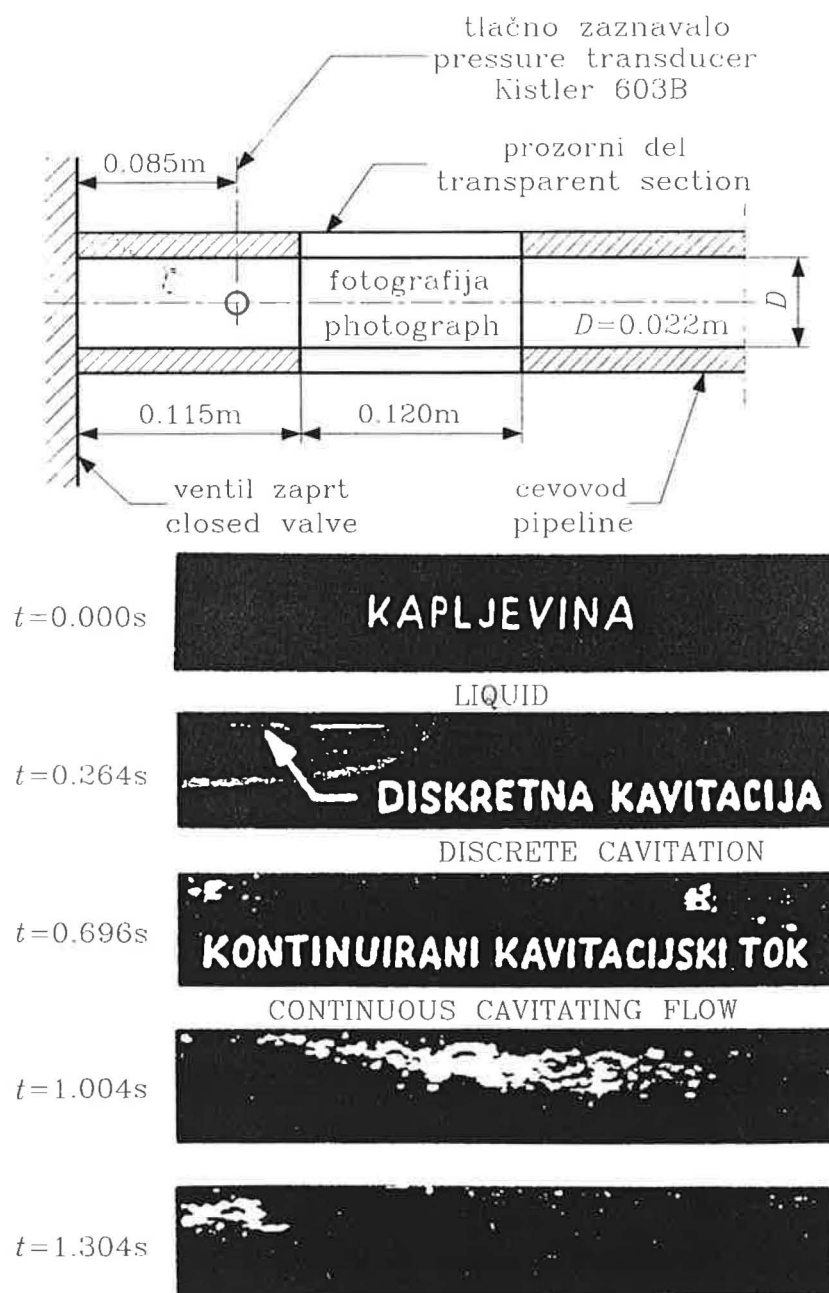
Sl. 4. Primerjava piezometričnih višin H_{mp} na polovici dolžine cevovoda
Fig. 4. Comparison of piezometric heads H_{mp} at the midpoint of the pipeline

in četrto pretrganje vodnega stebra pri ventilu se izmerjeni in izračunani časi obstoja kavitacije dobro ujemajo. Izračunani in izmerjeni tlačni sunki, ki zaporedno sledijo nastanku in zrušitvi diskretne kavitacije pri ventilu (sl. 3) in kondenzaciji kombiniranih področij kontinuirnega kavitačijskega toka in diskretnih kavitacij vzdolž cevovoda v kapljevinsko fazo (sl. 4), se ujemajo v zadovoljivi meri. Izračunana največja prostornina diskretnih kavitacij vzdolž cevovoda (red velikosti 10^{-8} do 10^{-8} m^3) je mnogo manjša od prostornine diskretne kavitacije pri ventilu (red velikosti 10^{-5} m^3). Največja prostornina diskretne kavitacije pri ventilu (V_v)_{dv} = $3.97 \times 10^{-5} \text{ m}^3$ je mnogo manjša od prostornine cevnega odseka $V = A\Delta x$ = $8.95 \times 10^{-4} \text{ m}^3$ (4.4 %).

difference. However, the measured and computed times agree well for the second, third and fourth lengths of cavity existence at the valve. There is reasonable agreement between the computed and measured pressure pulses following subsequent cavity collapse and reopening at the valve (Fig. 3) and condensation of combined discrete vapour cavities along the pipe line back to the liquid-phase (Fig. 4). The maximum volume of discrete cavities along the pipe line (of magnitude 10^{-8} to 10^{-8} m^3) is much less than the volume of the discrete cavity at the valve (of magnitude 10^{-5} m^3). The maximum volume of a discrete cavity at the valve (V_v)_{dv} = $3.97 \times 10^{-5} \text{ m}^3$ is much less than the pipe reaction volume $V = A\Delta x = 8.95 \times 10^{-4} \text{ m}^3$ (4.4 %).

Diskretno kavitacijo pri ventilu in področje kontinuiranega kavitacijskega toka vzdolž cevovoda smo razbrali tudi s hitro snemalnega videa Kodak Ektapro 1000 (poglavje 3). Razporeditev prozornega dela pri ventilu in fotografije kontinuiranega kavitacijskega toka za obravnavani preizkus so podane na sliki 5. Kapljevina na fotografiji je v črni barvi. Oblika prve kavitacije je bela, notranja prostornina kavitacije pa je temna. Kasnejše diskrette kavitacije pri ventilu in v področju kontinuiranega kavitacijskega toka so fotografirane v beli barvi. Ob vsaki fotografiji je podan čas od trenutka vzbuditve prehodnega pojava.

A discrete cavity at the valve, and distributed vaporous cavitation zone along the pipeline, was visually identified by Kodak Ektapro 1000 high-speed video photography (Section 3). Layout of the transparent section at the valve and photographs of the cavitating flow for the considered experiment are given in Fig. 5. The liquid is observed as black. The shape of the first cavity is identified as white. The internal volume of this cavity is observed as dark. The subsequent discrete cavities at the valve and in the distributed vaporous cavitation zones are observed as white. Each photograph shows the elapsed time from



Sl. 5. Vizualizacija kavitacijskih pojavov pri ventilu
Fig. 5. Visualisation of cavitation phenomena at the valve

Opazovana največja prostornina diskretne kavitacije pri ventilu se pojavi v času $t = 0,264$ s. Prva diskretna kavitacija ne zajame celotnega prečnega prereza cevovoda. Izračunana največja prostornina diskretne kavitacije pri ventilu se pojavi v času $t = 0,275$ s (razlika 4,2 %). V nadaljevanju prehodnega procesa se največja prostornina kavitacije pri ventilu zmanjšuje. Pretrganje vodnega stebra pri ventilu je turbulentno, vzdolž cevovoda pa razberemo področje kontinuiranega kavitacijskega toka. Področje kontinuiranega kavitacijskega toka je delno sklenjeno.

Sklepamo, da razlike med rezultati izračuna in meritev izvirajo iz približnega popisa kontinuirnega kavitacijskega toka z diskretnimi kavitacijami v numeričnem modelu [2], [4]. Odstopanja v manjši meri izvirajo tudi iz diskretizacije v numeričnem modelu ($\Delta t = L/(aN) = 37,2 / (1319 \times 16) = 0,00176$ s), aproksimacije neustaljenega koeficiente trenja kapljevine z ustaljenim Darcy-Wisbachovim koeficientom trenja λ [22] in pogreškov pri merivi [15]. Domnevamo, da oblika kavitacije ne vpliva na porast tlaka po zrušitvi kavitacije [8].

5 SKLEP

Meritve vodnega udara in pretrganja kapljivinskega stebra smo izvedli v preizkusni postaji. Ta je sestavljena iz 37,2 m dolgega poševnega cevovoda, ki je vgrajen med dva tlačna kotla. Prehodni pojavi so vzbujeni s hitrim zapiranjem ventila. Izmerjeni časovni potek tlaka in vizualizacija pretrganja kapljivinskega stebra s hitro snemalnim videom pomembno prispevata k boljšemu razumevanju fizikalnega pojava. Vizualizacija toka razkrije tip kavitacije in časovni potek dogodka. Izmerili in fotografirali smo diskretno parno kavitacijo in kontinuirni kavitacijski tok pri parnem tlaku kapljivine. Domnevamo, da oblika kavitacije ne vpliva na zvišanje tlaka po zrušitvi kavitacije. Rezultati izračuna z diskretnim plinskim kavitacijskim modelom se dobro ujema z rezultati meritev. V izračunu izbrani plinski kavitacijski razmernik $\alpha_0 = 10^{-7}$ je dovolj majhen za natančni izračun vodnega udara in simuliranje kavitacijskega toka med prehodnimi režimi v cevnih sistemih.

the initiation of the transient event. The visualised maximum discrete cavity volume at the valve appears at time $t = 0.264$ s. The first discrete cavity does not occupy the entire cross section of the pipe. The computed maximum cavity volume at the valve appears at time $t = 0.275$ s (a discrepancy of 4.2 %). The maximum cavity volume at the valve decreases at subsequent column separations. Liquid column separation at the valve is turbulent and the distributed vaporous cavitation zone is visually observed along the pipeline. The distributed vaporous cavitation zone is partially homogeneous.

In conclusion, the discrepancies between measured and computed results are contributed to the approximate simulation of distributed vaporous cavitation zones by discrete cavities [2], [4] within the model. In addition, the discrepancies also originate from discretisation of the computational model ($\Delta t = L/(aN) = 37.2 / (1319 \times 16) = 0.00176$ s), the unsteady friction term being approximated by the steady-state Darcy-Wisbach friction factor λ [22] and uncertainties in measurement [15]. The shape of the cavity does not seem to influence the pressure rise following cavity collapse [8].

5 CONCLUSION

Water-hammer and liquid column separation measurements were carried out in an experimental apparatus. The apparatus comprises a straight 37.2 m long sloping pipeline connecting two pressurised tanks. Transient events are initiated by rapid closure of a valve. Measured pressure versus time traces and observation via high-speed video photography has provided an improved understanding of liquid column separation phenomena. Flow visualisation detects the type of cavitation and time sequence of the events. The discrete vapour cavities and distributed vaporous cavitation zones were measured and observed in column separation tests. The shape of the cavity does not seem to influence the pressure rise following cavity collapse. The results of a discrete gas cavity model agree well with the results of measurement. The selected gas void fraction in the model $\alpha_0 = 10^{-7}$ is small enough for accurate water-hammer computation and simulation of transient cavitating flow piping systems.

li-
ve
ste
of
ne
s-
ne
e-
is
on
he
lly
he
ed
ed
es
s-
in
=
dy
dy
nd
of
s-
on
i-
a
ng
re
ed
by
an
a-
he
he
i-
ed
he
he
e-
ill
ed
ill
on
in

OZNAČBE

<i>A</i>	— prečni prerez,
<i>a</i>	— hitrost širjenja udarnih valov,
<i>D</i>	— premer cevovoda,
<i>f_s</i>	— frekvenca podatkov,
<i>g</i>	— zemeljski pospešek,
<i>H</i>	— piezometrična višina: $H = p / (\rho g) + z = h + z$,
<i>h</i>	— tlačna višina,
<i>h_v</i>	— parna tlačna višina,
<i>h₀*</i>	— absolutna referenčna tlačna višina,
<i>j</i>	— številka vozlišča,
<i>L</i>	— dolžina cevovoda,
<i>N</i>	— število cevnih odsekov,
<i>p</i>	— tlak,
<i>t</i>	— čas,
<i>t_c</i>	— čas zapiranja ventila,
<i>V</i>	— prostornina,
<i>v</i>	— pretočna hitrost, vstopna hitrost v vozlišče,
<i>v_u</i>	— izstopna hitrost iz vozlišča,
<i>x</i>	— koordinata,
<i>z</i>	— geodetska višina,
<i>α₀</i>	— plinski kavitacijski razmernik pri referenčni tlačni višini,
<i>β</i>	— potenca v enačbi τ ventila,
Δt	— časovni korak,
Δx	— dolžina cevnega odseka,
ϑ	— strmina cevovoda,
λ	— Darcy-Weisbachov koeficient trenja,
ρ	— gostota tekočine,
τ	— brezdimenzijski čas odprtja ventila,
ψ	— utežni koeficient.

INDEKSI

<i>dr</i>	— navzdolnji kotel,
<i>dv</i>	— ventil na navzdolnjem koncu,
<i>f</i>	— končna lega,
<i>g</i>	— plin,
<i>i</i>	— začetna lega,
<i>mp</i>	— polovica dolžine cevovoda,
<i>ur</i>	— navzgornji kotel,
<i>v</i>	— para,
<i>o</i>	— začetno stanje.

ZAHVALA

Raziskave pretrganja kapljevinskega stebra v cevnih sistemih je podprt Avstralski svet za raziskave, za kar se mu iskreno zahvaljujeva. Članek je bil napisan med obiskom dr. Berganta na Univerzi v Adelaidi, Avstralija. Avtorja izražata zahvalo vodstvu Litostroja, Slovenski znanstveni fundaciji, Ministrstvu za znanost in tehnologijo Slovenije in Univerzi v Adelaidi, ki so podprli ta obisk.

NOMENCLATURE

<i>A</i>	— pipe area,
<i>a</i>	— wave propagation velocity,
<i>D</i>	— pipe diameter,
<i>f_s</i>	— sampling frequency,
<i>g</i>	— gravitational acceleration,
<i>H</i>	— piezometric head: $H = p / (\rho g) + z = h + z$,
<i>h</i>	— pressure head,
<i>h_v</i>	— vapour pressure head,
<i>h₀*</i>	— absolute reference pressure head,
<i>j</i>	— node number,
<i>L</i>	— pipe length,
<i>N</i>	— number of reaches in pipeline,
<i>p</i>	— pressure,
<i>t</i>	— time,
<i>t_c</i>	— valve closure time,
<i>V</i>	— volume,
<i>v</i>	— flow velocity, downstream velocity at node,
<i>v_u</i>	— upstream velocity at node,
<i>x</i>	— distance,
<i>z</i>	— elevation,
<i>α₀</i>	— gas void fraction at reference pressure head,
<i>β</i>	— exponent in τ valve equation,
Δt	— time step,
Δx	— pipe reach length,
ϑ	— pipe slope,
λ	— Darcy-Weisbach friction factor,
ρ	— liquid density,
τ	— dimensionless valve opening,
ψ	— weighting factor.

SUBSCRIPTS

<i>dr</i>	— downstream reservoir,
<i>dv</i>	— downstream end valve,
<i>f</i>	— final position,
<i>g</i>	— gas,
<i>i</i>	— initial position,
<i>mp</i>	— midpoint of the pipeline,
<i>ur</i>	— upstream reservoir,
<i>v</i>	— vapour,
<i>o</i>	— initial condition.

ACKNOWLEDGEMENTS

Liquid column separation research in piping systems has been supported by the Australian Research Council, and its support is gratefully acknowledged. In addition, this paper was written during Dr. Bergant's visit to the University of Adelaide, Australia. The authors wish to thank Litostroj, the Slovenian Science Foundation, the Slovenian Ministry of Science and Technology and the University of Adelaide who supported this visit.

6 LITERATURA 6 REFERENCES

- [1] Wylie, E.B.—Streeter, V.L.: *Fluid Transients in Systems*. Prentice Hall, Englewood Cliffs, 1993.
- [2] Bergant, A.: Kavitacijski tok med prehodnimi režimi v cevnih sistemih. Doktorska disertacija, Fakulteta za strojništvo Univerze v Ljubljani (Transient Cavitating Flow in Piping Systems. Doctoral Thesis, Faculty of Mechanical Engineering at the University of Ljubljana), Ljubljana, 1992.
- [3] Bergant, A.—Simpson, A. R.: Interface Model for Transient Cavitating Flow in Pipelines. Proceedings of the International Conference on Unsteady Flow and Fluid Transients, HR/IAHR, Durham, 1992, 333–342.
- [4] Simpson, A. R.—Bergant, A.: Numerical Comparison of Pipe-Column-Separation-Models. *Journal of Hydraulic Engineering*, ASCE, Vol. 120, 1994/3, 361–377.
- [5] Blake, W. K.: *Mechanics of Flow-Induced Sound and Vibration. Volume 1 – General Concepts and Elementary Sources*. Academic Press, Orlando, 1986.
- [6] Duc, J.: Negative Pressure Phenomena in a Pump Pipeline. *Sulzer Technical Review*, Vol. 41, 1959/3, 3–12.
- [7] O'Neill, I. C.: Water-Hammer in Simple Pipe Systems. M. Sc. Thesis, University of Melbourne, Melbourne, 1959.
- [8] Li, W. H.—Walsh, J. P.: Pressure Generated by Cavitation in a Pipe. *Journal of the Engineering Mechanics Division*, ASCE, Vol. 90, 1964/EM6, 113–133.
- [9] Baltzer, R. A.: Column Separation Accompanying Liquid Transients in Pipes. *Journal of Basic Engineering*, ASME, Vol. 89, 1967/4, 837–846.
- [10] Safwat, H. H.: Photographic Study of Water Column Separation. *Journal of the Hydraulic Division*, ASCE, Vol. 98, 1972/HY4, 739–746.
- [11] Tanahashi, T.—Kasahara, E.: Comparisons between Experimental and Theoretical Results of the Water Hammer with Water Column Separation. *Bulletin of JSME*, Vol. 13, 1970/61, 914–925.
- [12] Nonoshita, T.—Matsumoto, Y.—Ohashi, H.—Kubota, T.: Model Analysis of Water Column Separation Accompanied with Swirl Flow. International Meeting on Hydraulic Transients with Column Separation, IAHR, Valencia, 1991, 235–249.
- [13] Swaffield, J. A.: A Study of Column Separation Following Valve Closure in a Pipeline Carrying Kerosene. *Proceedings of IME*, Vol. 184, 1969–70/3G(1), 57–64.
- [14] Kojima, E.—Shinada, M.—Shindo, K.: F Transient Phenomena Accompanied with Column Separation in Fluid Power Pipeline. *Bulletin of JSME*, Vol. 1984/233, 2421–2429.
- [15] Bergant, A.—Simpson, A. R.: Water-Hammer and Column Separation Measurements in an Experimental Apparatus. Research Report No. R128, Department of Civil and Environmental Engineering, University of Adelaide, Adelaide, 1995.
- [16] Coleman, H. W.—Steele, W. G.: *Experimental and Uncertainty Analysis for Engineers*. John Wiley Sons, New York, 1989.
- [17] Simpson, A. R.—Bergant, A.: Developments in Pipeline Column Separation Experimentation. *Journal of Hydraulic Research*, IAHR, Vol. 32, 1994/2, 183–194.
- [18] Merzkirch, W.: *Flow Visualisation*. Academic Press, Orlando, 1987.
- [19] Streeter, V. L.: *Water-Hammer Analysis*. Journal of the Hydraulic Division, ASCE, Vol. 95, 1969/1959–1972.
- [20] Provoost, G. A.—Wylie, E. B.: Discrete Model to Represent Distributed Free Gas in Liquids. *Proceedings of the 5th International Symposium on Column Separation*, IAHR, Obernach, 1981, 249–258.
- [21] Wylie, E. B.: Simulation of Vaporous Gaseous Cavitation. *Journal of Fluids Engineering*, ASCE, Vol. 106, 1984/3, 307–311.
- [22] Bergant, A.—Simpson, A. R.: Estimating Unsteady Friction in Transient Cavitating Pipe Flow. *Proceedings of the 2nd International Conference on Water Pipeline Systems*, BHR Group, Edinburgh, 1994, 3–16.
- [23] Bergant, A.—Simpson, A. R.: Quadratic Equation Inaccuracy for Water-Hammer. *Journal of Hydraulic Engineering*, ASCE, Vol. 117, 1991/11, 1572–1574.
- [24] Simpson, A. R.—Wylie, E. B.: Large Water-Hammer Pressures for Column Separation in Pipelines. *Journal of Hydraulic Engineering*, ASCE, Vol. 117, 1991/10, 1310–1316.

Naslova avtorjev: dr. Anton Bergant, dipl. inž.
Litostroj, tovarna turbin
Litostrojska 40
1515 Ljubljana

dr. Angus Simpson
Oddelek za gradbeništvo in
varstvo okolja
Univerza v Adelaidi
Južna Avstralija 5005

Authors' Addresses: Dr. Anton Bergant, Dipl. Inž.
Litostroj Turbine Factory
Litostrojska 40
1515 Ljubljana, Slovenia,

Dr. Angus Simpson
Department of Civil and
Environmental Engineering
University of Adelaide
South Australia 5005